

Journal of Nanophotonics

SPIDigitalLibrary.org/jnp

Subwavelength surface waves with zero diffraction

Juan J. Miret
David Pastor
Carlos J. Zapata-Rodríguez

Subwavelength surface waves with zero diffraction

Juan J. Miret,^a David Pastor,^b and Carlos J. Zapata-Rodríguez^b

^aUniversidad de Alicante, Departamento de Óptica, Farmacología y Anatomía, P.O. Box 99, Alicante, Spain

^bUniversidad de Valencia, Departamento de Óptica, Dr. Moliner 50, 46100 Burjassot, Spain
carlos.zapata@uv.es

Abstract. We identified nanostructured devices sustaining out-of-plane nondiffracting beams with near-grazing propagation and a transverse beamwidth clearly surpassing the diffraction limit of half a wavelength. This type of device consists of a planar multilayered metal-dielectric structure with a finite number of films deposited on a solid transparent substrate. We assumed that the nondiffracting beam is launched from the substrate. The construction of the subwavelength diffraction-free beam is attended by plane waves which are resonantly transmitted through the stratified medium. Therefore, light confinement and wave amplification occurs simultaneously. We performed an optimization process concerning the layers width as free parameters in order to reach the most efficient optical resonances with uniform transmission. The value of the propagation constant and the focal placement are initially arbitrary, which can be chosen according to its practical realization. Possible applications include optical trapping, biosensing, and nonlinear optics. © 2011 Society of Photo-Optical Instrumentation Engineers (SPIE). [DOI: [10.1117/1.3583989](https://doi.org/10.1117/1.3583989)]

Keywords: plasmonics; diffraction.

Paper 11013SSR received Feb. 4, 2011; revised manuscript received Apr. 1, 2011; accepted for publication Apr. 8, 2011; published online May 12, 2011.

1 Introduction

An emerging area of interest in applied physics is the development of fast optical devices based on surface plasmon polaritons (SPPs). The latter are hybrid modes consisting of collective electron oscillations in a metal with propagating electromagnetic surface waves.¹ Potential applications of plasmonics are widespread, including microcircuitry, biosensing, and imaging. Development of new metal-dielectric (MD) photonic components is a branch of major currently-ongoing research effort, which is crucially relying on the availability of new materials, new device designs, and new fabrications.

Due to the spatial confinement of energy on the subwavelength scale, the idea of exploiting plasmons as signal carriers have become of high importance, and experiments on a variety of metallic structures have been carried out.^{2,3} Here we put special emphasis on stratified MD media. Two main problems arise in using SPPs. One relies on dissipative effects that exhibit even good metals leading to a significantly short propagation distance. In order to provide an ideally infinite traverse, self-healing wave modes may be achieved by means of an optically feeding mechanism. This is found for instance in prism coupling to SPPs using attenuated total internal reflection in the Kretschmann and Otto configuration.³ The second problem refers to poor capacity of nondiffracting beams to be spatially confined over a given MD flat interface in spite of its high localization perpendicularly. Recently we have known of an attractive proposal consisting of setting an ultrathin, low-index, dielectric ridge deposited on a multilayer which can act as a waveguide for resonant surface waves.⁴

Previously we have shown that 1D lossless MD photonic crystals can sustain nondiffracting wavefields with a transverse beams size clearly surpassing the diffraction limit.⁵ Such a

subwavelength effect is due to the combination of two different mechanisms: 1. the formation of surface resonances in the MD interfaces and 2. the existence of transparency bands associated with high spatial frequency of the wave field. In this contribution we extend these results to a realistic nanostructured device including a finite number of layers and losses inside the metallic medium. For this purpose we propose a multilayered structure providing a wide spatial spectrum. Manipulating the angular spectrum of the wave field we are able to create a diffraction-free beam with transverse focus near the flat end surface of the structure. Potential applications in electron acceleration, biosensing, and optical trapping are envisioned.

2 Diffraction-Free Beams in Finite Planar Multilayered MD Structures

Prior to the analysis of wave propagation, let us start with a description of the nanostructured medium wherein a nondiffracting light beam is produced. The device consists of a planar MD multilayer with a finite number N of metallic films deposited over a solid substrate, as shown in Fig. 1(a). We assume that the MD interfaces lies parallel to the xz -plane. The stratified medium is characterized by a relative dielectric constant $\epsilon(y)$ in the form of a discrete function. Particularly it takes a value ϵ_s in the substrate, ϵ_m in the metallic films, and ϵ_d in the dielectric layers. Also d_m and d_d refer to the width corresponding to each metallic slab and each dielectric slab, respectively. Therefore our finite 1D photonic structure has a period $\Lambda = d_m + d_d$. Finally we consider dielectric ending layers of width $d_d/2$, which results in a higher performance as discussed elsewhere.^{6,7}

Next we consider a monochromatic vector beam propagating along the z -axis. For diffraction-free waves, the electromagnetic fields may be factorized into two functions. One depends on the transverse coordinates (x, y) and in general is different for every component of the vector fields. However the second function is set as a function of the axial coordinate z and it is common in all vector components. Specifically the electric and magnetic fields are written as

$$\vec{E}(x, y, z, t) = \vec{e}(x, y) \exp(i\beta z - i\omega t), \quad (1)$$

$$\vec{H}(x, y, z, t) = \vec{h}(x, y) \exp(i\beta z - i\omega t), \quad (2)$$

where ω is the frequency of the radiation and β is the propagation constant.

In order to excite surface resonances in the MD interfaces of our device, p -polarized waves should be employed. Therefore we consider TM waves in which the magnetic field is confined in the xz -plane, that is $\vec{h} = (h_x, 0, h_z)$. We point out that the electric field is obtained from \vec{h} by using the Maxwell equations, $\vec{E} = (i/\omega\epsilon_0)\nabla \times \vec{H}$, and that the magnetic field is solenoidal

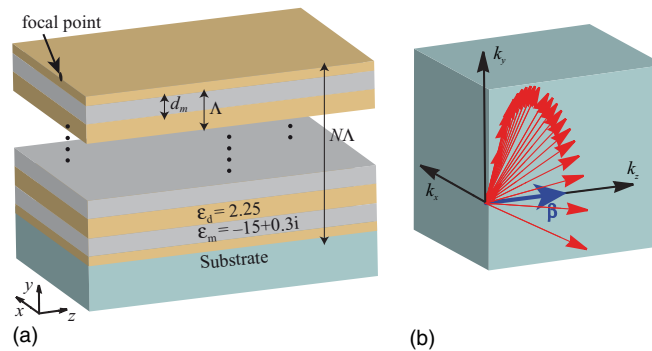


Fig. 1 (a) The multilayered structure composed of thin films of Ag and fused silica. (b) Wave-vector distribution of the NDB launched. This construction guarantees the nondiffractive character of the beam.

leading to the equation $h_z = i\beta^{-1}\partial_x h_x$. We conclude that our problem may be fully established in terms of the scalar wavefield h_x , from which all the other electromagnetic components may be derived.

From a practical point of view it is reasonable to assume that the nondiffracting beam (NDB) is launched from the substrate where we elude evanescent propagation [$\text{Re}(\epsilon_s) \gg 1$] and dissipative effects [$\text{Im}(\epsilon_s) = 0$]. By using the plane-wave expansion of the field h_x , the light beam in the substrate may be understood as the superposition of infinite plane waves in which the wave vector $\vec{k} = (k_x, k_y, k_z)$ projected onto the propagation axis z gives the characteristic propagation constant, $k_z = \beta$. This is illustrated in Fig. 1(b). In mathematical terms, the wave field directed toward the MD nanostructure may be written as

$$[h_x]_{\text{inc}} = \sum_{k_x} w(k_x) \exp(ik_x x + ik_y y), \quad (3)$$

where the transverse spatial frequency $k_y > 0$ is given by the dispersion equation $k_y^2 = k_0^2 \epsilon_s - \beta^2 - k_x^2$. In Eq. (3) we assume a superposition of a discrete number of plane waves for convenience, however it may be generalized straightforwardly to a continuous distribution.⁸ Finally $w(k_x)$ represents the strength of the spectral component with spatial frequency k_x in the plane-wave expansion (3).

In order to obtain the field distribution inside the MD structure we may consider individually every plane wave constituting the spectral components of Eq. (3). Boundary conditions lead to conservation of the wave field h_x over the MD interfaces, keeping the spatial frequencies β and k_x unaltered. The general procedure may be followed from Ref. 5. Note that using a standard matrix formulation for isotropic layered media⁹ we describe unambiguously the field distribution $w(k_x) \exp(ik_x x) \tilde{h}(k_x, \beta, y)$ generated inside our device by a plane wave of transverse spatial frequency k_x and strength $w(k_x)$ launched from the substrate. Finally, the wave field h_x characterizing the NDB is set in terms of the summation $\sum_{k_x} w(k_x) \exp(ik_x x) \tilde{h}(k_x, \beta, y)$.

In general, the superposition of plane waves proposed in Eq. (3) cannot generate a localized wave field inside the MD device. Therefore some favorable requisites must be established in order to form a line focus parallel to the z -axis around a given transverse point $P_0 = (x_0, y_0)$. For that purpose we manipulate the relative phases between different plane-wave components in order to reach the same argument of the spectral field at the geometric focus P_0 . Thus the oscillatory superposition yields the highest intensity achievable. Moreover, under ordinary conditions a point other than P_0 cannot be found contained in the xy -plane where such a phase matching holds. As a consequence, a strong confinement of the NDB is expected to occur around P_0 . In this paper we impose phase matching at a point P_0 placed on the uppermost MD interface as shown in Fig. 1(a). Also we consider a uniform source distribution of plane waves leading to the condition $|w(k_x)| = 1$.

3 Response of MD Nanostructures in Space and Frequency Domains

Next we briefly discuss some aspects on wave propagation in MD periodic nanostructures of finite size in order to describe appropriate conditions for the formation of subwavelength NDBs inside. For the sake of clarity we consider a MD multilayered medium composed of 10 thin metallic films of width $d_m = 25$ nm separated by a distance $\Lambda = 425$ nm and embedded in a nonabsorbing dielectric medium of $\epsilon_d = 2.25$. The periodic structure is deposited onto a transparent solid substrate with dielectric constant $\epsilon_s = 3.7$ and covered by air ($\epsilon = 1.0$). We consider silver layers of $\epsilon_m = -15 + i0.3$ at a wavelength $\lambda_0 = 550$ nm.¹⁰

We evaluate the spatial distribution of the wave field inside the MD device produced by different plane waves launched from the substrate. Obviously we primarily focus on the excitation of spatial frequencies k_x belonging to transparency bands in the 1D photonic crystal so that we also include the computation of the transmission coefficient from the front end joining the substrate up to the back-end surface. In Fig. 2(a) we show a log plot of the transmission coefficient

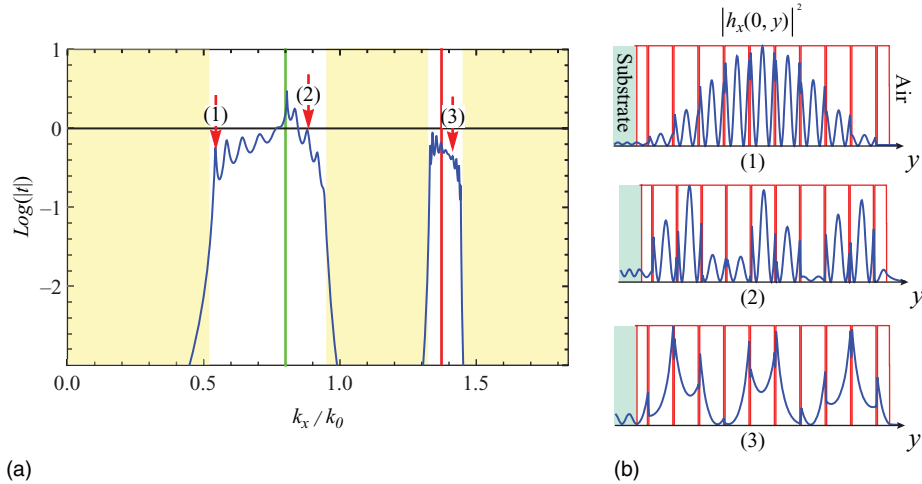


Fig. 2 (a) Transmission coefficient of the multilayer device composed of 10 thin films of Ag ($\epsilon_m = -15 + i0.3i$) and dielectric medium ($\epsilon_d = 2.25$) with widths $d_m = 25$ nm and $d_d = 400$ nm, respectively. The high-index substrate is transparent ($\epsilon_s = 3.7$) and the covering medium is air. Shaded regions correspond to the forbidden bands of the infinite MD structure. (b) Field intensity along the y -axis for plane waves with spatial frequency k_x (1), (2), and (3) pointed in (a).

in modulus for the MD device described above. Here the transmission coefficient t accounts for the ratio of the field h_x at the output surface and the field $[h_x]_{\text{inc}}$ impinging from the substrate. Note that $|t|$ might be higher than unity. For illustration we consider a propagation constant $\beta = 0.6k_0$ in the numerical simulation, where $k_0 = 2\pi/\lambda_0$ is the wavenumber in vacuum. The transverse spatial frequency is simply the square root of $k_x^2 + \beta^2$. The existence of transparency bands concurs with allowed bands characteristic of the infinite MD photonic crystal as expected. Moreover high transmission peaks emerge from these spectral bands which are attributed to optical resonances of a different nature. We point out that a low value of the propagation constant β is associated with a wide spatial spectrum of k_x , which helps us to excite the largest variety of these transmission resonances as it happens with $\beta = 0.6k_0$.

In order to elucidate the origin of these optical resonances we have highlighted the frequencies $0.8k_0$ and $1.375k_0$, which are labeled with a solid light (green in color) line, and a dark (red in color) line, respectively. The frequency $k_x = 0.8k_0$ leads to a transverse spatial frequency coinciding with the wavenumber k_0 in air, whereas the frequency $k_x = 1.375k_0$ does it for a transverse spatial frequency $\sqrt{\epsilon_d}k_0$. Below the light line, the wavefields are of propagating nature in all dielectrics including the air and the resonances that appear here are simply Fabry–Pérot (FP) resonances. For the peaks within this spectral band, the Bloch wavenumbers k_B of the infinite 1D nanostructure satisfy the FP condition $k_B N \Lambda = m\pi$ being m a positive entire number.¹¹ In Fig. 2(a) the spatial frequency (1), $k_x = 0.536k_0$, is associated with a FP resonance of index $m = 1$. We also plot the normalized intensity pattern generated inside the MD structure as shown in Fig. 2(b). Note that the envelope accommodates the spatial distribution of a standing wave.

When the spatial frequency goes between the light line and the dark line in Fig. 2(a), as $k_x = 0.875k_0$ denoted by (2), the wavefields are evanescent in the air but they maintain their propagating character in the dielectric media. In this case the resonances are ascribed to the phenomenon known as optical resonant tunneling.⁹ It occurs when the incident plane wave is capable of exciting 1D bound states in the dielectric slabs of the structure. This involves the excitation of coupled planar waveguide modes in the transparent thin layers as may be identified in Fig. 2(b).

The peaks in transmittance beyond the dark line are still attributed to optical resonant tunneling. This is the case of $k_x = 1.425k_0$ tagged by (3) in Fig. 2(a). However the wave is clearly inhomogeneous both in the metal and in the dielectric layers [see Fig. 2(b)]. Also

the intensity reaches significantly high values in the MD interfaces suggesting the excitation of surface resonances. Therefore the tunneling effect is here sustained by coupled surface plasmons.^{12,13}

We point out that this type of plasmonic wave fields are attractive for us since they contain high frequencies along the x -axis and exhibit a rapid decay in the y -axis leading to ultra-localization in the transverse xy -plane. Moreover, for a given coupled plasmon resonance, wave confinement in the upper MD interface may go with higher intensities in adjacent surfaces. We have observed that the use of half-width dielectric layers at the ends of the MD device alleviates such a damaging effect for our purposes.^{6,7}

4 Numerical Results

In previous studies we showed that the contribution in the focus generation of all Bloch modes included in allowed bands of an infinite periodic MD structure leads to a transverse spotlight with a full width at half maximum (FWHM) that might surpass the diffraction limit.^{5,14} Next, if we consider a finite size of the MD device, the up-and-down behavior in transmission seen in Sec. 3 is expected to restrict the contribution of some spatial frequencies k_x and to stimulate some others which are related with peak resonances. In practice, Eq. (3) may include only those plane waves demonstrating high-efficiency transmission across the multilayered MD structure. Additionally this procedure allows us to simplify the evaluation of the transverse pattern characterizing the wave field inside the photonic lattice.

Let us consider some figures of merit that the MD structure should satisfy in order to optimize the formation of a tightly-focused NDB. First, large allowed bands would lead to high transmittance of the plane waves launched from the substrate. In fact the use of a continuous distribution of plane waves would become effective under flat transmissions. However numerous peaks attributed to resonances commonly comes out. Assuming that the peak transmittance is inhomogeneous we may modify $|w(k_x)|$ included in the discrete summation of Eq. (3) in order to control the field distribution in the vicinities of focus. However we seek for uniform peak responses and therefore we consider $|w(k_x)| = 1$ for simplicity. Finally a high cutoff spatial frequency k_x would let us construct spatial distributions with extremely narrow peaks along the x -axis.¹⁵

In order to optimize our MD device, we start by considering again silver ($\epsilon_m = -15 + 0.3i$) and fused silica ($\epsilon_d = 2.25$) layers deposited onto a solid transparent substrate of $\epsilon_s = 4.2$. Monochromatic plane waves of wavelength $\lambda_0 = 550$ nm are also assumed. In the search of a response following the criteria of large allowed bands, high cutoff spacial frequency, and numerous resonances with somehow similar transmission, we finally obtained $d_m = 25$ nm and $d_d = 160$ nm. This procedure ensures a suitable behavior for a moderate and high number N of metallic layers.

In Fig. 3(a) we represent the response in transmission of a MD device composed of $N = 5$ metallic layers. In order to get rid of resonances of the FP type, we will not consider $\beta = 0.6k_0$ which is employed in Fig. 2. Alternatively the propagation constant is increased up to $\beta = k_0$. This leads to inhomogeneous waves in air for $k_x \neq 0$. The arrows point to resonance peaks associated with discrete values of k_x used in the generation of the NDB. The transverse distribution of intensity computed for a NDB with focus located on the center of the uppermost MD interface is plotted in Fig. 3(b). An NDB with an anamorphic focal spot of subwavelength beamsizes given by FWHMs $\Delta_x = 132$ nm and $\Delta_y = 40.6$ nm is obtained. We point out that the value of Δ_y is similar to that encountered in the SPP generated by a single silver-fused silica interface at our wavelength ($\Delta_y = 40$ nm). Importantly, the intensity reached at focus is 5.2 times higher than that encountered by the in-phase interference of plane waves given in Eq. (3) performed in the substrate. Therefore light confinement and wave amplification occurs simultaneously.

Increasing the number N of metallic layers also leads to an increment in the number of transmittance peaks, which is attributed to the generation of high-order plasmonic modes.¹⁶

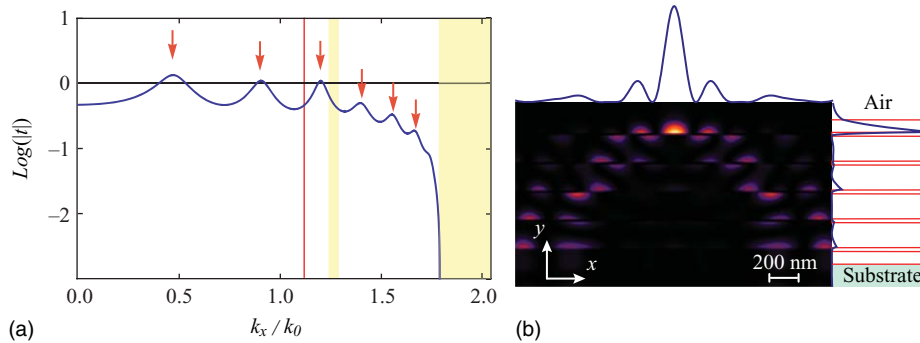


Fig. 3 (a) Transmission coefficient for a MD structure as shown in Fig. 1 with $N = 5$ silver layers of width $d_m = 25$ nm immersed in fused silica ($\Lambda = 185$ nm). The arrows mark the positive values of the spatial frequencies k_x used in the focal construction developed in Eq. (3). (b) Intensity pattern of the NDB in the xy -plane.

Considering $N = 10$ the NDB achieves a hot spot with $\Delta_x = 116$ nm and $\Delta_y = 39.9$ nm (see Fig. 4). In comparison with the previous case the value of the FWHM along the y direction remains roughly the same. This is explained by the plasmonic nature of the wave field near the geometrical focus. On the other hand an enhanced resolution is observed along the x direction due to the increment of the spectral components in Eq. (3) and their corresponding frequencies k_x . Unfortunately dissipative effects become severe and the peak intensity is only 2.7 times that encountered in an isotropic medium.

Note that finite thickness of the substrate would modify the transmission coefficient t and thus the distribution of peak resonances. Therefore experimental demonstrations of our ultraconfined NDBs should consider such a circumstance. Nevertheless the results presented here could still be valid even in this case. Reflections at the new entrance surface are potentially compensated by tailoring the strength $|w(k_x)|$ of the wave field. As a consequence the focal distribution would be unaltered near the exit surface.

Finite size of plane waves may impose further restrictions for an adequate formation of a transverse focus. It is well documented that beam truncation also circumscribes the effective propagation distance along which the NDB is maintained unaltered.^{17,18} The latter effect however is not discussed in this paper. In Fig. 5 we plot the spatial distribution of the NDB sustained by the MD multilayered structure obtained from a numerical experiment performed with a commercial finite-element package (COMSOL Multiphysics). Note that we performed 2D

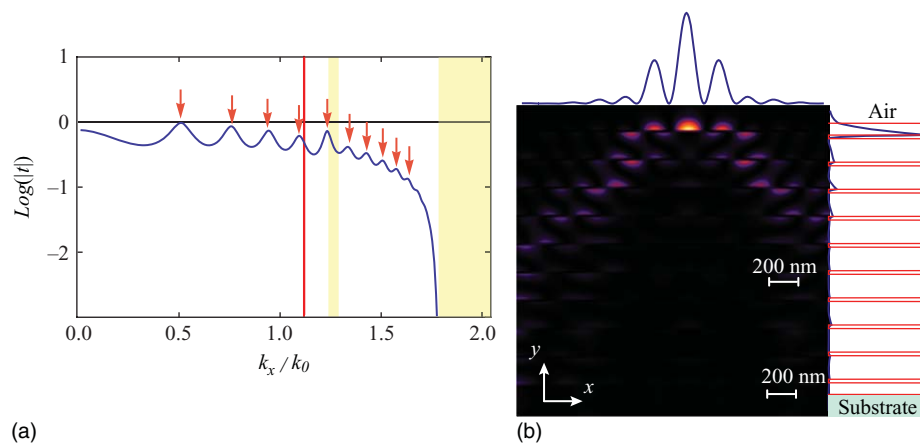


Fig. 4 The same as in Fig. 3 but using $N = 10$ Ag films. In this case we have a profit from 10 resonances associated with positive values of k_x .

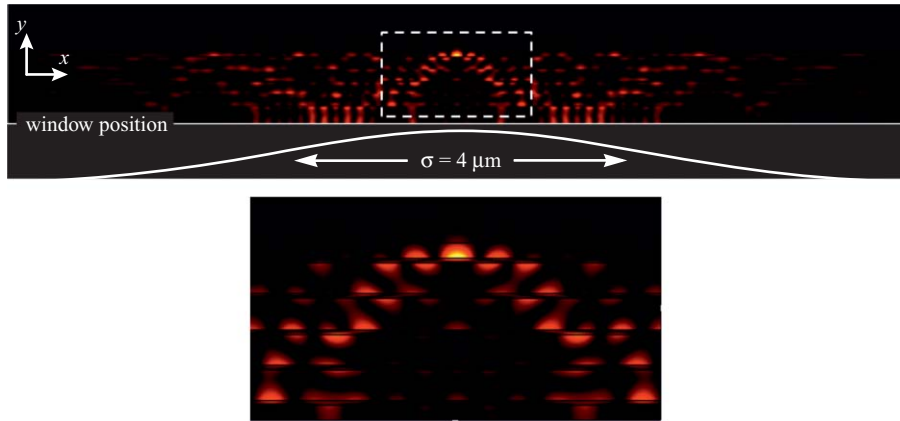


Fig. 5 Numerical experiment performed with COMSOL Multiphysics.

simulations, however, the wave equation was modified in order to include an on-axis spatial frequency β . That is, our wave fields are 2D in intensity but they include a factor $\exp(i\beta z)$ in their amplitudes. In this experiment we have considered a MD device of $N = 5$ silver films and the same opto-geometric characteristics used in Fig. 3. Following a semi-realistic model, every infinitely-uniform plane wave is substituted here by a Gaussian wave of transverse and on-axis spatial frequencies k_x and β , respectively, whose intensity distribution includes a factor $\exp(-x^2/\sigma^2)$, being the Gaussian width $\sigma = 4 \mu\text{m}$. The one-dimensional Gaussian window coincides for every spectral component of the incident wave field, which is placed beside the front-end surface of the MD photonic device, as labeled in Fig. 5. We confirm the validity of our previous results given in Fig. 3(b). In spite of using a considerably narrow Gaussian window including high-angle spectral components, we form a subwavelength NDB propagating over the uppermost MD interface. Spurious light out of the boxed region decreases in intensity due to the finite magnitude of the impinging field along the x direction, which might become a beneficial effect for most potential applications.

5 Conclusions

We have identified a nanostructured device that can sustain diffraction-free beams with near-grazing propagation and with transverse beamsizes clearly surpassing the diffraction limit of half a wavelength. This device consists of a planar multilayered MD structure with a finite number of layers deposited on a solid substrate. We illuminate from the substrate with a set of TM-polarized monochromatic plane waves all having a wavevector that projected onto the z -axis gives the characteristic propagation constant β . We select the spectral components as those that are more efficiently transmitted across the nanophotonic structure.

We also consider realistic material losses in the numerical simulations. The strength of every incident wave is uniform whereas their relative phases are chosen in order to achieve a phase matching at a given focal point. As a consequence, a strong localization of the NDB is demonstrated to occur around the focus.

In the numerical simulation we have selected a NDB with propagation constant coinciding with the wavenumber in vacuum and a focal point placed on the uppermost MD interface, however other values of β and focal placements are available. Light confinement and wave amplification occurs simultaneously, which may have potential applications in nonlinear optics. In waveguide-based biosensing, these structures might provide new opportunities for applications in which the waveguide is made out of functionalized molecular layers of nanometric thicknesses. Other applications include microlithography, optical micromanipulation, and electron acceleration.

Acknowledgments

This research was funded by Ministerio de Ciencia e Innovación (MICIIN) under the project TEC2009-11635.

References

1. H. Raether, *Surface Plasmons on Smooth and Rough Surfaces and on Gratings*, Springer-Verlag, Berlin (1988).
2. S. A. Maier and H. A. Atwater, "Plasmonics: Localization and guiding of electromagnetic energy in metal/dielectric structures," *J. Appl. Phys.* **98**(1), 011101 (2005).
3. S. A. Maier, *Plasmonics: Fundamentals and Applications*, Springer, New York (2007).
4. T. Sfez, E. Descrovi, L. Yu, D. Brunazzo, M. Quaglio, L. Dominici, W. Nakagawa, F. Michelotti, F. Giorgis, O. J. F. Martin, and H. P. Herzig, "Bloch surface waves in ultrathin waveguides: Near-field investigation of mode polarization and propagation," *J. Opt. Soc. Am. B* **27**, 1617–1625 (2010).
5. J. J. Miret and C. J. Zapata-Rodríguez, "Diffraction-free propagation of subwavelength light beams in layered media," *J. Opt. Soc. Am. B* **27**(7), 1435–1445 (2010).
6. M. Scalora, M. J. Bloemer, A. S. Pethel, J. P. Dowling, C. M. Bowden, and A. S. Manka, "Transparent, metallo-dielectric, one-dimensional, photonic band-gap structures," *J. Appl. Phys.* **83**, 2377–2383 (1998).
7. S. Feng, M. Elson, and P. Overfelt, "Transparent photonic band in metallodielectric nanostructures," *Phys. Rev. B* **72**, 085117 (2005).
8. C. J. Zapata-Rodríguez and J. J. Miret, "Diffraction-free beams in thin films," *J. Opt. Soc. Am. A* **27**, 663–670 (2010).
9. P. Yeh, *Optical Waves in Layered Media*, Wiley, New York (1988).
10. P. B. Johnson and R. W. Christy, "Optical constants of the noble metals," *Phys. Rev. B* **6**(12), 4370–4379 (1972).
11. P. A. Belov, C. R. Simovski, and P. Ikonen, "Canalization of subwavelength images by electromagnetic crystals," *Phys. Rev. B* **71**, 193105 (2005).
12. S. Feng, J. M. Elson, and P. L. Overfelt, "Optical properties of multilayer metal-dielectric nanofilms with all-evanescent modes," *Opt. Express* **13**, 4113–4124 (2005).
13. M. Scalora, G. D'Aguanno, N. Mattiucci, M. J. Bloemer, D. de Ceglia, M. Centini, A. Mandatori, C. Sibilia, N. Akozbek, M. G. Cappeddu, M. Fowler, and J. W. Haus, "Negative refraction and sub-wavelength focusing in the visible range using transparent metallo-dielectric stacks," *Opt. Express* **15**, 508–523 (2007).
14. J. J. Miret and C. J. Zapata-Rodríguez, "Diffraction-free beams with elliptic Bessel envelope in periodic media," *J. Opt. Soc. Am. B* **25**, 1–6 (2008).
15. M. Martínez-Corral, P. Andrés, C. J. Zapata-Rodríguez, and M. Kowalczyk, "Three-dimensional superresolution by annular binary filters," *Opt. Commun.* **165**, 267–278 (1999).
16. S. M. Vukovic, Z. Jaksic, and J. Matovic, "Plasmon modes on laminated nanomembrane-based waveguides," *J. Nanophoton.* **4**, 041770 (2010).
17. J. Durnin, J. J. Miceli, and J. H. Eberly, "Diffraction-free beams," *Phys. Rev. Lett.* **58**, 1499–1501 (1987).
18. G. Indebetouw, "Nondiffracting optical fields: Some remarks on their analysis and synthesis," *J. Opt. Soc. Am. A* **6**, 150–152 (1989).

Biographies and photographs of the authors not available.